

Molecular motion of poly(methyl methacrylate) chains tethered on a polyethylene surface by the spin-label method

Shigetaka Shimada*, Masato Kozakai and Katsuhiko Yamamoto

Nagoya Institute of Technology, Gokiso-cho, Showa-ku, Nagoya 466, Japan

(Received 1 September 1997; revised 7 January 1998; accepted 27 January 1998)

Methyl methacrylate monomer was graft-copolymerized on a polyethylene (PE) surface and the tethered poly(methyl methacrylate) (PMMA) chains were spin-labelled to study the molecular motion of the PMMA chains by electron spin resonance (e.s.r.).

Molecular mobility of the PMMA chains is strongly affected by physical structures of both PE and PMMA phases. For example, the transition temperature of molecular motion, $T_{5.0 \text{ mT}}$, at which the extreme separation width due to ^{14}N anisotropic hyperfine splitting is 5.0 mT, increases with increases in the grafting ratio and the crystallinity of the PE phase. The transition temperature for the grafted sample is lower than that for PMMA homopolymer bulk and the mobility of the PMMA chains in the mobile region of the grafted sample is much higher than that of PE chains on the PE surface. It is concluded that the structure and molecular motion of the PMMA chains tethered on the PE surface are strongly affected by the PE chains in the amorphous phase, the structure and molecular motion of which are also closely related to the crystallinity and/or the size of crystalline PE. © 1998 Elsevier Science Ltd. All rights reserved.

(Keywords: tethered chains; poly(methyl methacrylate); polyethylene)

INTRODUCTION

We have studied the structure and molecular motion of polymer chains tethered on poly(tetrafluoroethylene) (PTFE)^{1–3} and adsorbed on porous silica surfaces^{4,5} by the spin label method. The high mobility of the tethered polymer chains was found and related to the extremely low segmental concentration. When one end of the polymer chains is fixed on the surfaces, the aggregation behaviours of the polymer chains are much different from those for the homopolymer chains, both ends of which are free. Then, the loosely packed structure of the tethered chains may grow even for the samples with the high grafting ratio.

Another interesting problem is the effect of the base polymer on the molecular motion of the tethered chains.

In this paper, we prepare the samples of the poly(methyl methacrylate) (PMMA) grafted on a polyethylene (PE-g-PMMA) with a wide range of grafting ratios. We will clarify the molecular motion of the PMMA chains tethered on the PE surface as a function of the grafting ratio, related to segmental density and molecular mobility of the PE chains, and discuss a mechanism for the aggregation of the tethered PMMA chains.

EXPERIMENTAL

Materials

A high-density linear polyethylene (HDPE) (Sholex6050, Showa Denko Co. Ltd) and a low-density branched polyethylene (LDPE) (Sumikathene G-20, Sumitomodenko Co. Ltd) were purified three times by dissolving them in boiling toluene, then precipitated by cooling and washing in

acetone. The purified powder samples were dried in a vacuum oven for a long time. The average diameter of the powder particles was *ca.* 0.7 mm. Next, the samples were irradiated with ^{60}Co γ -ray at room temperature in air. The total dose was *ca.* 16.1 kGy at a dose rate of 0.336 kGy h⁻¹. Methylmethacrylate (MMA) monomer (Nacalai Tesque Co. Ltd) was purified by a freeze–pump–thaw method. Atactic PMMA with a weight-average molecular weight of 83 000 and a polydispersity of 1.85 (Aldrich Chemical Co., Inc.) was purified by dissolving it in acetone, precipitating it in excess methanol, and filtering. This procedure was repeated three times. The PMMA powder sample was then dried *in vacuo* at room temperature for 2 days.

Preparation of PMMA chains tethered on PE surface

The irradiated PE samples were placed in glass tubes and degassed. After the introduction of MMA monomers to these glass tubes, these were sealed and placed at 343 ± 0.5 K. The graft copolymerization was initiated by radicals, $-\text{CH}_2-\text{C}(\text{O})-\text{CH}_2-$, produced by decomposition of peroxide, $-\text{CH}_2-\text{C}(\text{OOH})-\text{CH}_2-$ ⁶, on the PE surface. The grafting ratio was a function of storage time at 343 K. After the copolymerization, unreacted monomer and PMMA homopolymer were extracted with acetone using a Soxhlet apparatus and the sample was completely dried *in vacuo* at room temperature for 2 days. The grafting ratio of each sample was determined by the gravimetric measurement. Grafting ratio(%) = (PMMA fraction(g)) \times 100/(PE fraction(g)).

Spin-labelling

The tethered PMMA chains and the PMMA homopolymer were spin labelled by amide–ester interchange

* To whom correspondence should be addressed

reaction with 2,2,6,6-tetramethyl-4-aminopiperidine-1-oxy(4-amino-TEMPO) (Aldrich Chemical Co. Ltd) in methanol containing sodium methoxide^{7,8}. The labelled samples were repeatedly dispersed in CH₃OH-H₂O and filtered to remove the large amount of unreacted spin-label reagents. This procedure was repeated more than six times. As discussed in the previous paper, the PMMA chains on the surface of the bulk were selectively spin-labelled because the reaction was performed in poor solvent for PMMA³.

In order to study a surface molecular mobility of PE⁹, mechanical fracture of the PE powder as purified with 2,4,6-tri-*tert*-butyl nitrosobenzene (BNB, Sigma. Chem. Co. Ltd) was carried out by milling in a home-made vibration glass ball mill *in vacuo* at room temperature for 36 h.

Electron spin resonance measurements

The samples were stacked in the electron spin resonance measurement (e.s.r.) sample tubes and evacuated to 10⁻⁵ Torr before e.s.r. measurement. Electron spin resonance measurement spectra at 77 K and higher temperatures were observed at a low microwave power level to avoid power saturation and with 100 kHz fielded modulation using JEOL JES-FE3XG and JES-RE1XG spectrometers (X band) coupled to microcomputers (NEC PC 9801). The signal of diphenylpicrylhydrazyl (DPPH) was used as a *g*-value standard. The magnetic field sweep was calibrated with known splitting constants of Mn²⁺.

Differential scanning calorimetry measurements. Differential scanning calorimetry (d.s.c.) measurements were carried out using a Rigaku DSC 8230L differential scanning calorimeter. Differential scanning calorimetry curves were run at 10°C min⁻¹.

X-ray diffraction measurements. X-ray diffraction measurements were carried out using a Rigaku RINT-1100 with CuK α ($\lambda = 1.5405$ Å) equipment.

RESULTS AND DISCUSSION

Surface molecular mobility of PMMA homopolymer

In our previous paper³, the spin-label method was used to study the surface molecular mobility of PMMA homopolymer bulk. Figure 1 shows e.s.r. spectra of spin-labelled PMMA (SL-PMMA) in the PMMA homopolymer, observed at various temperatures. In general, the outermost splitting width of the main triplet spectrum due to hyperfine coupling caused by the nitrogen nucleus narrows with an increase in mobility of the radicals because of motional averaging of the anisotropic interaction between electron and nucleus. The complete averaging gives rise to the isotropic narrowed spectrum. The extreme separation width between arrows indicated in Figure 1 gradually narrows and steeply drops with an increase in temperature. The temperature dependence of the extreme separation width for the PMMA sample is shown in Figure 2. The steep drop is caused by a micro Brownian type molecular motion¹⁰⁻¹². We estimate a transition temperature of molecular motion, $T_{5.0 \text{ mT}}$, at which an extreme separation width is equal to 5.0 mT.

First, e.s.r. measurements were carried out with warming of the sample (increasing temperature). Next, the sample was cooled after annealing at 473 K, and e.s.r. measurements were carried out with decreasing temperature. The spectral changes in Figure 1 were completely reversed on cooling, and all the spectra were exactly reproduced at

particular temperatures upon repetition of the heat-cool cycle. On the other hand, the molecular mobility of the SL-PMMA located on the interior region was compared with the surface molecular mobility in our previous paper. The temperature dependence of the extreme separation width for the spin-label is also shown in Figure 2 (dotted curve), and $T_{5.0 \text{ mT}}$ is found to be 440 K, 30 K higher than that of the spin-label on the surface region³.

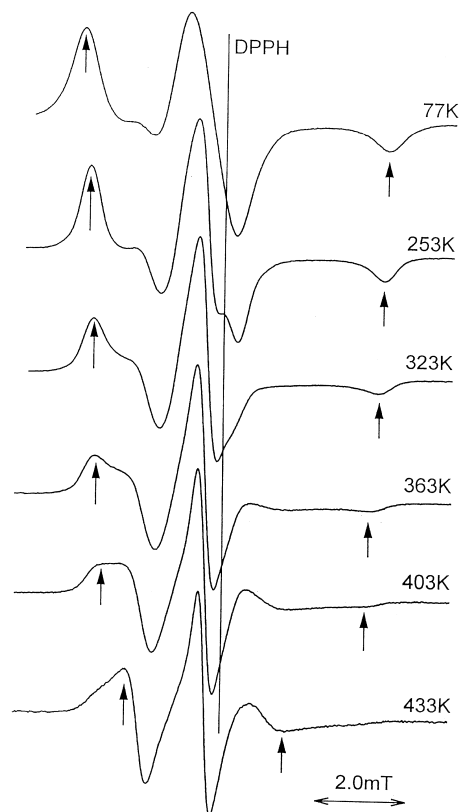


Figure 1 Temperature-dependent e.s.r. spectra of SL-PMMA in PMMA homopolymer bulk. The separation between arrows shows the extreme separation width

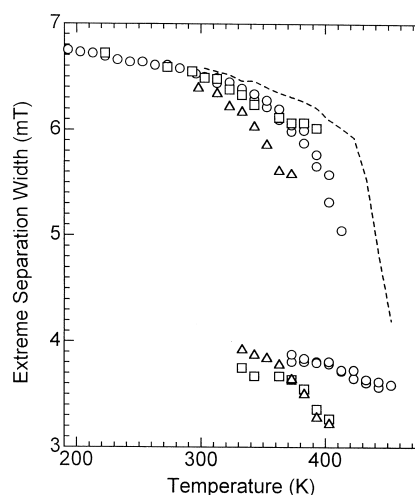


Figure 2 Temperature dependences of the extreme separation width for SL-PMMA in the PMMA homopolymer bulk (○) and in the PE-g-PMMA samples with the grafting ratios of 14.1% (Δ) and 352% (□). The dotted curve indicates the temperature dependence for the SL-PMMA located in the interior region of the PMMA homopolymer bulk³. E.s.r. measurements were carried out with increasing temperature

Surface molecular mobility of PE homopolymer

Figure 3 shows the variation in e.s.r. spectra of spin-labelled PE(HDPE) (SL-PE) with temperature. It is well known that mechano radicals are trapped on the fresh surface generated by the mechanical fracture¹³. Many kinds of spin-adducts were produced by reactions of the spin trapping agent, BNB with the mechano radicals under vacuum at room temperature. The e.s.r. spectrum observed at 403 K can be assigned to be a mixture of the primary and secondary nitroxide radicals and anilino radicals¹⁴⁻¹⁷. In the present paper, the anilino-type radicals, peaks of which are indicated by arrows in Figure 3, are used as a spin-label to study molecular motion of PE chains in the amorphous region of the PE surface. As the size of the anilino radical is of the same order of magnitude as that of the spin-label

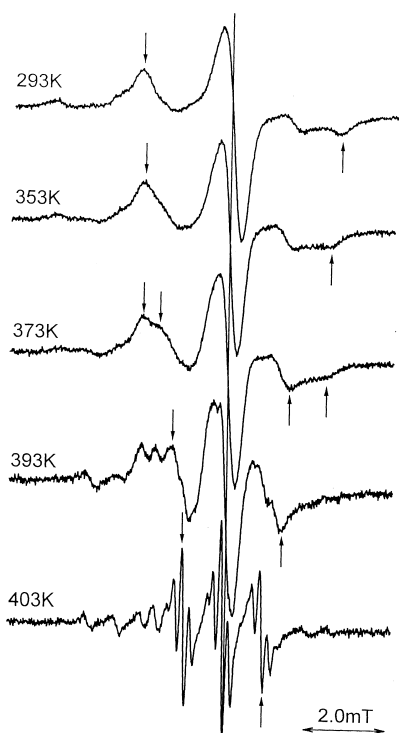


Figure 3 Temperature-dependent e.s.r. spectra of SL-PE on the PE surface

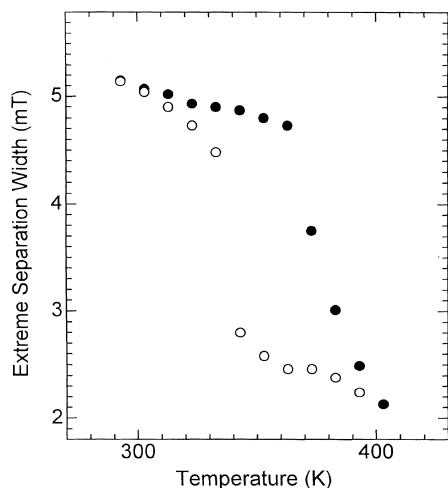


Figure 4 Temperature dependences of the extreme separation width for SL-PE: heating (●); cooling (○)

bonded to the PMMA chain, we can compare reasonably the molecular mobility of PE chains with that of PMMA chains by the e.s.r. method. The extreme separation widths for the spin-labels are plotted against temperatures in Figure 4. The width decreases gradually and steeply drops at 373 K with increasing temperature. The steep drop is also caused by a micro-Brownian-type molecular motion. The transition appears at a higher temperature than the glass transition temperature of PE because of a higher frequency of e.s.r. spectroscopy¹⁰⁻¹². The transition temperature of the surface molecular motion of PE can be estimated to be 373 K. The curve of the extreme separation width shifts *ca.* 35 K to a low-temperature side when e.s.r. experiments are performed with cooling of the same sample after heat treatment at 403 K for a long time. PE crystals are melted by the heat treatment. The crystallinity of PE is lower on the cooling process than that on the heating process. Exactly the same experiments were carried out using the LDPE sample with much lower crystallinity (37%) than that (66%) of the HDPE sample. The extreme separation width steeply drops at 335 K, which is 40 K lower than that for the HDPE sample. The curve also shifts *ca.* 15 K to a low temperature side when e.s.r. experiments are performed with cooling after the heat treatment at 403 K. These experimental facts suggest that the molecular mobility of PE in the amorphous region near the surface increases with a decrease in crystallinity of PE.

Molecular mobility of tethered PMMA chains on the PE surface

Figures 5 and 6 show temperature dependences of e.s.r. spectra of spin-labelled PMMA (SL-PMMA) tethered on the PE(HDPE) surface with the grafting ratios of 14.1% and 352%, respectively. First, e.s.r. measurements were carried out with warming of the sample (increasing temperature). Next, the sample was cooled after the heat treatment at 403 K, and e.s.r. measurements were carried out with decreasing temperature. The temperature dependences of the extreme separation width for the grafted samples are also shown in Figure 2. The transition temperature seems to increase with an increase in grafting ratio. It can be considered that the grafted PMMA chains are phase-separated on the PE phase because of their immiscibility with the PE chains. The SL-PMMA should be also located on the PMMA phase as discussed in the previous section. The following results are found from the temperature dependences.

Dependence of molecular mobility on mole fraction of PMMA. Two spectral components, a 'fast' and a 'slow' component, are observed in a certain temperature range. The slow component with large outermost splitting width and the fast component with small outermost splitting width and narrow line width can be attributed to radicals in the rigid and mobile regions, respectively. The two spectral components are observed in a wide temperature range for the grafted sample. This is a reflection of a distribution of correlation time¹⁸ arising from a heterogeneous structure of the tethered chains on the PE surface. For example, the distributions of molecular weight, segmental density and free volume of the tethered chains can be considered to be broad. The intensities of the fast component for the sample with the grafting ratio of 14.1% are larger than those for the sample with the grafting ratio of 352%, as shown in Figures 5 and 6 (see, for example, the spectra at 383 K for the heating process). The line width of the 'fast'

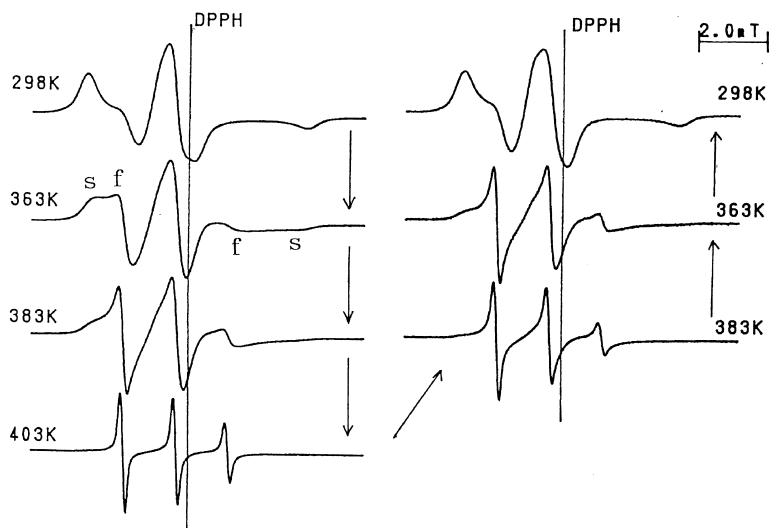


Figure 5 Temperature-dependent e.s.r. spectra of SL-PMMA on the PE surface with the grafted ratio of 14.1%. The arrows between the spectra indicate routes on which e.s.r. spectra were observed. Fast and slow components are indicated by 'f' and 's', respectively

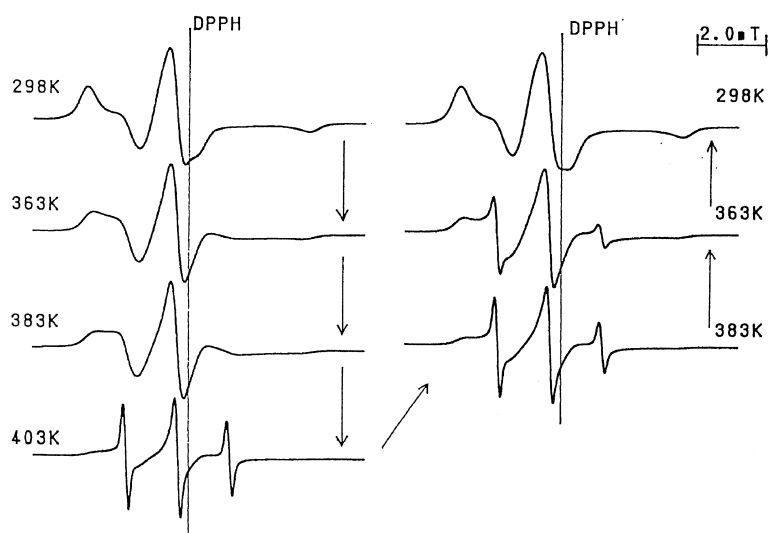


Figure 6 Temperature-dependent e.s.r. spectra of SL-PMMA on the PE surface with the grafting ratio of 352%. The arrows between the spectra indicate routes on which e.s.r. spectra were observed

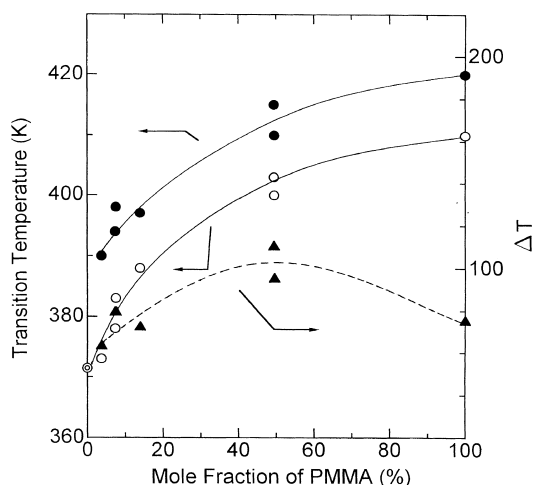


Figure 7 Dependences of transition temperatures, $T_{5.0 \text{ mT}}$ (○) and T_H (●) and the difference, $\Delta T(\blacktriangle) = T_H - T_L$ on the mole fraction of PMMA. The mark ⊙ is the transition temperature of the molecular motion of PE estimated from the curve in Figure 4. The e.s.r. measurements were carried out with increasing temperature

component's spectrum for the grafted chains is extremely narrow in comparison with that for the PMMA homopolymer bulk (see, for example, the spectra at 403 K in Figures 1, 5 and 6). These facts suggest that the molecular mobility of the tethered PMMA chains is very high and has a strong dependence on the grafting ratio.

The $T_{5.0 \text{ mT}}$ obtained from the temperature dependences of the extreme separation width of the slow component for the grafted samples with various grafting ratios is plotted against the mole fraction of PMMA in Figure 7. However, the determination of the $T_{5.0 \text{ mT}}$ in Figure 2 is subjective because of coexistence of the two spectral components. Then, two characteristic temperatures, T_L and T_H , were estimated. The lower T_L is where the sharp ^{14}N isotropic triplet spectrum first appears as the sample is warmed, while the upper T_H is where the broad spectrum identified with the anisotropic pattern finally disappears. The difference between T_L and T_H , ΔT , was also estimated as a measure of the distribution of molecular mobility. The method for the determination of the characteristic temperatures is mentioned in detail in our previous paper³. The T_H and

ΔT obtained are also plotted against the mole fraction of PMMA in *Figure 7*. The temperatures $T_{5.0\text{ mT}}$ and T_H drastically increase until *ca.* 10 mole%, and gradually increase with an increase in mole fraction of PMMA. The extrapolated temperature of the $T_{5.0\text{ mT}}$ to 0 mole fraction of PMMA is approximately consistent with the transition temperature (373 K) of the molecular motion of spin-labelled PE on the PE(HDPE) surface. Exactly the same experiments were carried out using the LDPE sample with much lower crystallinity than that of the HDPE sample. The temperatures $T_{5.0\text{ mT}}$ of the spin-labelled PMMA on the PE(LDPE) surface are lower than those for the HDPE sample. The extrapolated temperature of the $T_{5.0\text{ mT}}$ to 0 mole fraction of PMMA is also approximately consistent with the transition temperature (335 K) of the surface molecular motion of the LDPE sample. In the previous section, it could be concluded that the molecular mobility of PE in the amorphous region near the surface was strongly affected by the crystallinity of PE. These experimental facts suggest that the grafted PMMA chains should be tethered on the PE surface and the molecular motion of the PMMA chains is strongly affected by the PE chains in the amorphous phase.

Difference between molecular mobility of PMMA chains near the surface and in the interior region on the PMMA phase. In order to compare the molecular mobility of the PMMA segments near the surface region with that in the interior region, an additional experiment was executed. The sample with the grafting ratio of 352% was swelled in benzene and precipitated in methanol. By this procedure, some SL-PMMA segments located near the surface of the PMMA phase should diffuse into the interior region. The temperature dependence of the extreme separation width for the sample was shown in *Figure 8* and compared with the result for the PMMA homopolymer bulk. The curve for the segments of the tethered SL-PMMA in the interior region shifts *ca.* 30 K to a lower temperature side in comparison with that for the chains in the surface region. This change is the opposite of the change for the PMMA homopolymer bulk discussed in our previous paper³. This experimental fact suggests that the mobile PE chains accelerate the

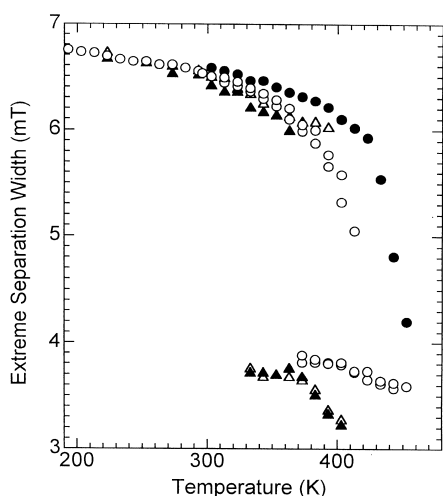


Figure 8 Temperature dependences of the extreme separation width for SL-PMMA near the surface (Δ) and interior (\blacktriangle) regions of the PMMA phase for the PE-g-PMMA sample with 352% of grafting ratio, compared with those for SL-PMMA near the surface (\circ) and interior (\bullet) regions of PMMA homopolymer bulk

molecular motion of the tethered PMMA segments in the interior region near the PE surface to more mobile chains than those near the PMMA surface, which are distant from the PE surface. The structural difference between the segments near the surface and interior regions of the PMMA phase is schematically depicted in *Figure 9a* as a difference of free volume. The T_L for the grafted sample is much lower than the transition temperature for the PE chains on the PE surface. For example, the T_L for the sample with a low grafting ratio of 14.1% is 55 K lower than the transition temperature of the PE chains—373 K. This fact can be interpreted in terms of the extremely low segmental density in the mobile region of the PMMA surface. The surface structure should grow during the graft copolymerization. The ΔT increases with an increase in mole fraction of PMMA. This reflects that the amount of the PMMA chains on the PE surface increases, the inhomogeneous structures of the surface develop, and the PMMA chains have a wide distribution of molecular mobility. Surprisingly, the molecular motion of the tethered PMMA chains is rapid (T_H and $T_{5.0\text{ mT}}$ is low) and the surface structure is inhomogeneous (ΔT is large), even for the sample with a large mole fraction of 50% in comparison with those for the PMMA homopolymer bulk. This should be caused by the development of aggregation of the PMMA chains under fixing of one end of the chains to the PE surface.

Studies on surface structure and the surface molecular motion of polymer materials have been carried out by many workers^{19,20}. The glass transition temperature of polymer segments at the surface region is lower than that for the polymer bulk. The larger free volume at the surface region compared with that in the interior region would be due to the localized chain end group at the surface region²¹. When one end of each PMMA chain is fixed to the PE surface, the tethered PMMA chains cannot behave as Gaussian chains, but as a polymer brush²². Then, the other ends of the polymer chains have more intensive distribution at the surface region than that for the PMMA homopolymer bulk. The inhomogeneous structure of the tethered PMMA chains is also schematically shown in *Figure 9*.

Dependence of molecular mobility on crystallinity of PE. The spectra in *Figures 5 and 6* differ, unlike the spectra in *Figure 1*, at any temperatures, depending on whether they were recorded on the heating or cooling part of the cycle (see, for example, the two spectra at 363 K in *Figure 5*). The intensity of the fast component on cooling is larger than that on heating. Indeed, during the heat treatment of the grafted sample at 403 K, the system should approach a thermodynamic equilibrium at the same temperature.

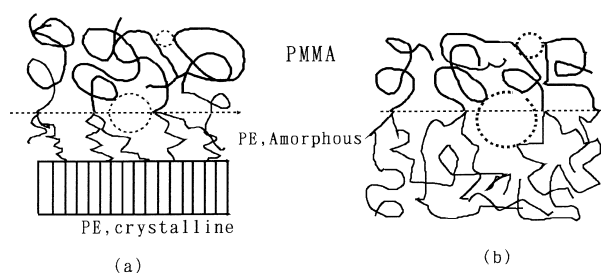


Figure 9 A schematic model of surface structure of grafted PMMA on the PE surface: (a) as-prepared sample; (b) (a) is heated above the melting point of PE

Figure 10 shows a variation in the e.s.r. spectrum of SL-PMMA chains tethered on the PE surface with annealing. First, the sample with the grafting ratio of 266% was stored at 373 K and the spectrum of Figure 10a was observed at the same temperature. Next, the sample was annealed at the desired temperature above 373 K for 30 min, cooled to 373 K and e.s.r. measurements were carried out at the same temperature. The procedure was repeated many times with increasing annealing temperature. It is found that the fast-motion component which has a narrow line width appears drastically at 393–403 K, and the variation of the spectrum is not observed above the temperatures with increasing temperature. It is well known that the melting point of PE crystal is around 403 K. These facts suggest that the molecular motion of the PMMA chains tethered on the PE surface should be

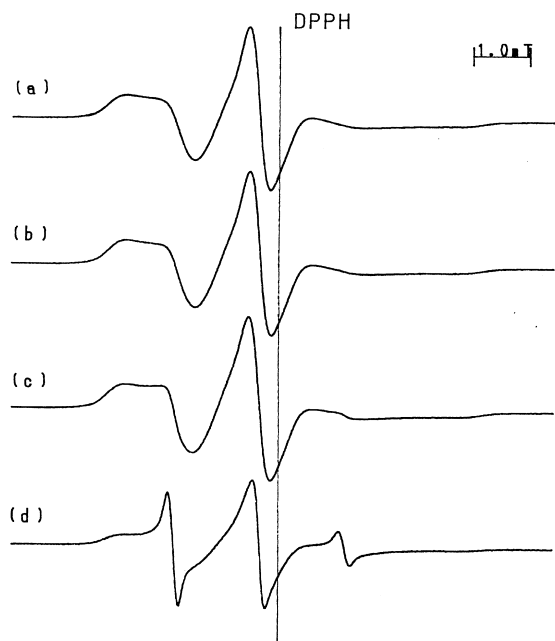


Figure 10 Variation of e.s.r. spectra of SL-PMMA tethered on the PE surface with the grafting ratio of 266% with annealing. The e.s.r. measurements were carried out at 373 K before (a) and after annealing at 383 K (b), 393 K (c) and 403 K (d)

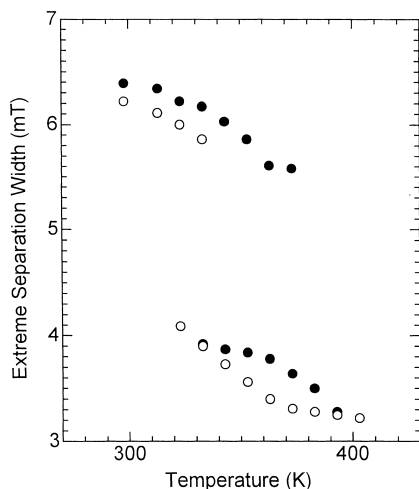


Figure 11 Temperature dependences of the extreme separation width for SL-PMMA near the PE surface with the grafting ratio of 14.1%: heating (●); cooling (○)

strongly affected by the crystallinity and/or the crystal size of PE. Figure 11 shows a comparison of the temperature dependence of the extreme separation width for heating process with that for the cooling process for the SL-PMMA tethered on the PE surface with the grafting ratio of 14.1%. It is found that the curve shifts ca. 40 K to a lower temperature side when e.s.r. measurements are carried out with cooling. The remarkable hysteresis was observed for all grafted samples. The transition temperature, $T_{5.0 \text{ mT}}$, T_H , and the difference, ΔT are increasing functions of mole fractions, as indicated in Figure 12. The temperatures, $T_{5.0 \text{ mT}}$ and T_H increase linearly with an increase in mole fraction of PMMA, in contrast to the results before the heat treatment (Figure 7). The extrapolated temperature of T_H to 0 mole fraction of PMMA is also consistent with the transition temperature (338 K) of molecular motion of SL-PE on the PE surface after the heat treatment above the melting point of the PE crystal. The T_L for the grafted sample is lower than that for the SL-PE on the PE surface and much lower than that for the SL-PMMA on the PMMA homopolymer bulk. These facts are similar to the results obtained for the heating process, except for the shifts of the transition temperatures to low temperatures. The differences, ΔT , are smaller than those before the heat treatment. (Compare Figure 12 with Figure 7.) This suggests that the surface structure approaches a uniform one. On the other hand, the linear dependences of $T_{5.0 \text{ mT}}$ and T_H on the mole

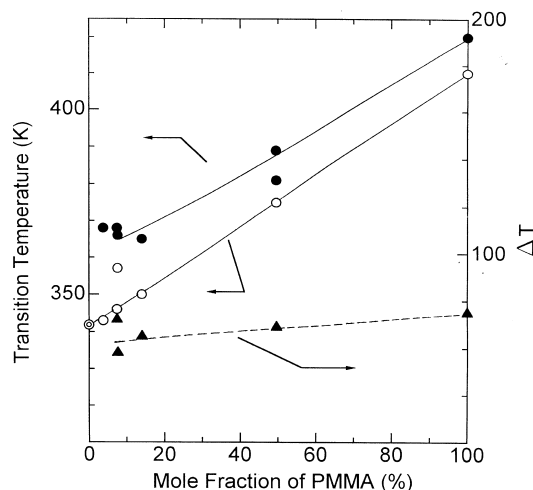


Figure 12 Dependences of transition temperatures, $T_{5.0 \text{ mT}}$ (○) and T_H (●), and the difference, ΔT (▲) = $T_H - T_L$, on the mole fraction of PMMA. The mark ⊙ is the transition temperature of the molecular motion of PE estimated from the curve in Figure 4. The e.s.r. measurements were carried out with decreasing temperature

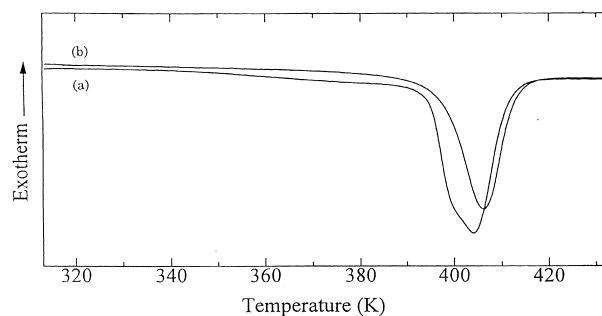


Figure 13 D.s.c. traces of the PE-g-PMMA with the grafting ratio of 352%: (a) the first heating; (b) the second heating

Table 1 The crystallinity and the lamellar dimension of the grafted sample with the grafting ratio of 81.9% by means of d.s.c. and X-ray diffraction (XRD), respectively (see text)

	Heat of fusion (J g ⁻¹) (d.s.c.)	Crystallinity (%)	Half width (degree) (XRD)	Lamellar dimension (Å)
Non-heat treatment	190	66	0.42	193
Heat treatment	167	57	0.87	93

fraction of PMMA suggest that the molecular mobility of the PMMA segments near the surface of the PMMA phase is approximately proportional to the distance between the PMMA surface and the PE-PMMA interface in the uniform structure. Because the distance should be also proportional to the mole fraction of PMMA, the spin labels are trapped near the surface of the PMMA phase.

Figure 13 shows d.s.c. traces of the sample of PE-g-PMMA with 352% of the grafting ratio. The crystallinity of PE phase can be obtained by taking 289 J/g²³ as the enthalpy of fusion of crystalline PE. The enthalpy of fusion for the second heating is smaller than that for the first heating, because the crystallinity of the PE phase decreases with heat treatment above the melting point of the PE crystal. The decrease in the crystallinity of the PE phase with the heat treatment becomes remarkable with an increase in grafting ratio. This result suggests that the PE chains cannot move rapidly to crystallize because the grafted PMMA chains slow down the molecular motion of the PE molecules. Table 1 indicates the crystallinity and the lamellar dimension of the grafted sample with the grafting ratio of 81.9% by means of d.s.c. and X-ray diffraction, respectively. The lamellar dimensions, $\langle l_{110} \rangle$, with some errors can be calculated from the half width of the X-ray diffraction pattern of PE crystals for the Miller index (110) by using the Sherrer equation²⁴. The remarkable increase in the half width with the heat treatment above the melting point of the PE crystal also indicates the decrease in the lamellar dimension of PE crystal. The decreases in crystallinity and crystal size are caused by a hindrance of the grafted chains from the crystallization of PE chains.

From these facts, it can be concluded that the structure and the molecular motion of the PMMA chains tethered on the PE surface are strongly affected by the crystallinity and/or the crystalline state, such as the crystal size of PE. The PMMA chains should be bonded to PE chains in the amorphous phase, which covers the PE crystal. The molecular mobility of PE in the amorphous phase is also strongly affected by the amount of crystal and the crystal size because the chains are constrained by the crystals of PE. Fixing of one end of each PMMA chain on the PE surface gives rise to a very different structure of the PMMA phase from the homopolymer bulk, and then the physical structures of PE should relate to the molecular motion of the PMMA chains. These effects of physical properties of

PE on the molecular motion of the tethered PMMA chains are also shown schematically in Figure 9.

CONCLUSIONS

1. Molecular mobility of PMMA chains tethered on PE surface decreases with increases in both mole fraction of PMMA and the crystallinity of the PE phase.
2. Fixing of one end of each PMMA chain on the PE surface gives rise to a very different structure of the PMMA phase, which has a large free-volume and a broad distribution in comparison with the PMMA homopolymer bulk.

ACKNOWLEDGEMENTS

The authors are grateful to Professor Sakaguchi (Ichimura Gakuene College) for helpful discussion.

REFERENCES

1. Sakaguchi, M., Yamaguchi, T., Shimada, S. and Hori, Y., *Macromolecules*, 1993, **26**, 2612.
2. Shimada, S., Suzuki, A., Sakaguchi, M. and Hori, Y., *Macromolecules*, 1996, **29**, 973.
3. Yamamoto, K., Shimada, S., Tsujita, Y. and Sakaguchi, M., *Macromolecules*, 1997, **30**, 1776.
4. Shimada, S., Sugimoto, A. and Kawaguchi, M., *Polymer*, 1997, **38**, 2251.
5. Shimada, S., Hane, Y. and Watanabe, T., *Polymer*, 1997, **38**, 4667.
6. Mukherjee, A. K. and Gupta, B. D., *J. Macromol. Sci. Chem.*, 1983, **A19**, 1069.
7. Baltzly, R., Berger, I. M. and Rothstein, A. A., *J. Amer. Chem. Sci.*, 1950, **72**, 419.
8. Vekslı, Z., Moller, W. G. and Thomas, E. L., *J. Polym. Sci. Symp.*, 1976, **54**, 299.
9. Sakaguchi, M. and Kashiwabara, H., *J. Polym. Sci. Polym. Phys. Ed.*, 1981, **19**, 371.
10. Shimada, S. and Kashima, K., *Polymer J.*, 1996, **28**, 690.
11. Sohma, J. and Sakaguchi, M., *Adv. Polym. Sci.*, 1978, **20**, 109.
12. Kusumoto, N., Sano, S., Zaitu, N. and Motozato, Y., *Polymer*, 1976, **17**, 448.
13. Tsay, F. and Gupta, A., *J. Polym. Sci. Polym. Phys. Ed.*, 1987, **25**, 855.
14. Terabe, S. and Kotaka, R., *J. Amer. Chem. Sci.*, 1971, **93**, 4306.
15. Shimada, S., Hori, Y. and Kashiwabara, H., *Macromolecules*, 1988, **21**, 2107.
16. Qu, B. J., Xa, Y. J., Shi, W. F. and Ranby, B., *Macromolecules*, 1992, **25**, 5215.
17. Qu, B. J., Xa, Y. J., Shi, W. F. and Ranby, B., *Macromolecules*, 1992, **25**, 5220.
18. Cameron, G. G., Miles, I. S. and Bullock, A. T., *Br. Polym. J.*, 1987, **19**, 29.
19. Kajiyama, T., Tanaka, K. and Takahara, A., *Macromolecules*, 1995, **28**, 3482.
20. Mayes, A. M., *Macromolecules*, 1992, **25**, 7317.
21. Tanaka, K., Taura, A., Ge, S.-R., Takahara, A. and Kajiyama, T., *Macromolecules*, 1996, **29**, 3040.
22. Milner, S. T., *Science*, 1991, **251**, 905.
23. Bandrup, J. and Halboth, E. H., *Polymer Handbook*, 2nd edn. Wiley-Interscience, New York, 1975.
24. Wireson, A., Lindberg, K. T. and Albertsson, A. C., *Polymer*, 1996, **37**, 761.